AD_____

Award Number: W81XWH-091-0183

TITLE: Targeting mrtl to Reverse Myc in Breast Oncogenesis

PRINCIPAL INVESTIGATOR: Scott Blume, M.D.

CONTRACTING ORGANIZATION: University of Alabama at Birmingham
Birmingham, Alabama 35294

REPORT DATE: June 2011

TYPE OF REPORT: Annual

PREPARED FOR: U.S. Army Medical Research and Materiel Command
Fort Detrick, Maryland 21702-5012

DISTRIBUTION STATEMENT: Approved for Public Release;
Distribution Unlimited

# REPORT DOCUMENTATION PAGE

*Form Approved*
*OMB No. 0704-0188*



| 1. REPORT DATE | 2. REPORT TYPE | 3. DATES COVERED |
|---|---|---|
| June 2011 | Annual | 1 June 2010 – 31 May 2011 |

**4. TITLE AND SUBTITLE**

Targeting mrtl to Reverse Myc in Breast Oncogenesis

**5a. CONTRACT NUMBER**

**5b. GRANT NUMBER**
W81XWH-09-1-0183

**5c. PROGRAM ELEMENT NUMBER**

**6. AUTHOR(S)**

Scott Blume, M.D.

**E-Mail:** scott.blume@ccc.uab.edu

**5d. PROJECT NUMBER**

**5e. TASK NUMBER**

**5f. WORK UNIT NUMBER**

**7. PERFORMING ORGANIZATION NAME(S) AND ADDRESS(ES)**

University of Alabama at Birmingham
Birmingham, Alabama 35294

**8. PERFORMING ORGANIZATION REPORT NUMBER**

**9. SPONSORING / MONITORING AGENCY NAME(S) AND ADDRESS(ES)**
U.S. Army Medical Research and Materiel Command
Fort Detrick, Maryland 21702-5012

**10. SPONSOR/MONITOR'S ACRONYM(S)**

**11. SPONSOR/MONITOR'S REPORT NUMBER(S)**

**12. DISTRIBUTION / AVAILABILITY STATEMENT**
Approved for Public Release; Distribution Unlimited

**13. SUPPLEMENTARY NOTES**

**14. ABSTRACT**

Our lab has discovered a 15 kDa protein, designated mrtl (myc-related translation / localization regulatory factor), which is generated from the same mRNA as c-Myc. We found that mrtl may be capable of direct interaction with the c-myc mRNA, and that ectopic overexpression of mrtl is associated with loss of Myc from the nucleus. Based on these results, we hypothesized that: (a) mrtl may regulate Myc translation and localization to the nucleus; and (b) mrtl may be a significant contributor to Myc-associated breast oncogenesis. Our experimental approaches include expression of wild-type or mutant mrtl in cis to Myc, and assessment of the consequences for Myc translation. We are examining mrtl and Myc in a series of human breast surgical specimens ranging from non-malignant to primary breast tumors to metastatic lesions of breast tumor origin, and investigating how the Myc IRES and differential expression of the p64 and p67 isoforms may ultimately determine the malignant phenotype. The results are helping to elucidate the functional relationship between mrtl and Myc, and the involvement of mrtl in development and progression of human breast cancer.

**15. SUBJECT TERMS**
Myc, mrtl, breast cancer, metastasis, polymorphism

| 16. SECURITY CLASSIFICATION OF: | | | 17. LIMITATION OF ABSTRACT | 18. NUMBER OF PAGES | 19a. NAME OF RESPONSIBLE PERSON |
|---|---|---|---|---|---|
| a. REPORT | b. ABSTRACT | c. THIS PAGE | | | USAMRMC |
| U | U | U | UU | 31 | 19b. TELEPHONE NUMBER *(include area code)* |

**Table of Contents**

**Page**

INTRODUCTION:

Our lab has discovered a 15 kDa protein, designated mrtl (*myc*-related translation / localization regulatory factor), which is generated from the same mRNA as c-Myc (1). There is no overlap or homology between these two proteins, i.e. mrtl is not an isoform of Myc. Although the mrtl (ORF1) reading frame had been recognized for a number of years, the natural existence of this hypothetical protein had not previously been established, and its function had not been investigated. The natural synthesis of mrtl in *cis* from the c-*myc* mRNA inherently places mrtl in the immediate vicinity of the regulatory sequences controlling the efficiency of Myc translation. We found that mrtl is closely associated with translation initiation factors (colocalization and co-IP), shares homology with a number of RNA-binding proteins (BLAST analyses), and may be capable of direct interaction with the c-*myc* mRNA sequence (northwestern). Furthermore, mrtl is prominently positioned throughout the nuclear envelope and the nucleoplasmic reticulum. We found that ectopic overexpression of mrtl was associated with a dramatic loss of Myc from the nucleus. Based on these results, we hypothesized that: (a) mrtl may regulate Myc translation and localization to the nucleus; (b) mrtl may be a significant contributor to Myc-associated breast oncogenesis; and (c) that a therapeutic intervention designed to interfere with mrtl function might be used to modulate Myc and reverse the malignant phenotype. This project is designed to further investigate the functional relationship between mrtl and Myc and to elucidate the possible involvement of mrtl in development and progression of human breast cancer. Our experimental approaches include ectopic expression of *wild-type* or mutant mrtl in *cis* to Myc, and assessment of the consequences for Myc translation and nuclear translocation. Through these experiments, we are attempting to elucidate the physiological mechanisms by which mrtl regulates Myc expression and function and influences proliferation of human breast tumor cells in culture. Based on their close genomic relationship, it is reasonable to anticipate that pathological alterations involving mrtl could be directly responsible for dysregulation of Myc in a proportion of human breast tumors. This project provides an opportunity to examine mrtl for the first time, at both the molecular and cellular levels, in primary breast tumor specimens.

**BODY:**

**Task 1: Determine whether mrtl modulates Myc translational efficiency in cis by influencing the internal ribosomal entry site.**

A major objective of this work was the development of two complex series of expression / reporter constructs which would allow us to investigate in detail the functional relationship between mrtl and Myc. In one series, epitope tags would be incorporated into both the mrtl and Myc coding sequences, allowing us to distinguish the ectopically produced proteins from endogenous Myc or mrtl. This would be particularly important because we suspect that the special genomic relationship between mrtl and Myc, in which mrtl is generated from the same mRNA molecule as Myc, might be critical for the regulatory influence of mrtl on Myc. Consequently, ectopically-produced mrtl might be expected to have a substantially greater effect on ectopically produced Myc (in *cis*) than on endogenous Myc (in *trans*). In the second series of constructs, the Myc coding sequence would be replaced in its entirety by the firefly luciferase coding sequence, allowing highly sensitive reporter analyses to be performed.

Throughout both series of constructs, we had elected to include as great a proportion of the natural sequence context of the human c-*myc* locus as possible (see schematic in **Figures 1A and B**), covering

approximately 8.1 kb of genomic sequence (Gazin et al (2), GenBank Accession X00364), in order to maximize the potential for recapitulating physiological Myc regulation and the mrtl / Myc relationship.

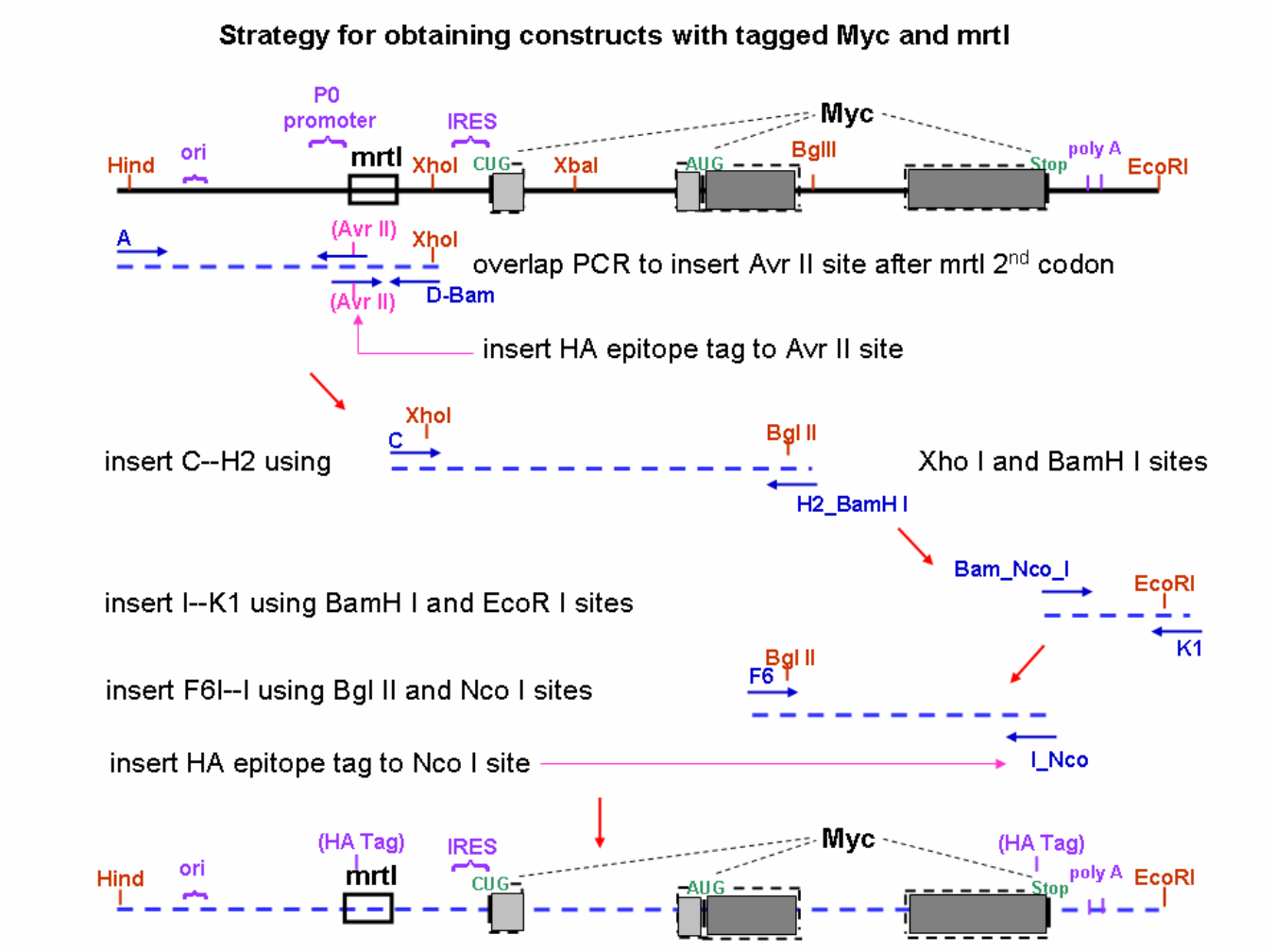

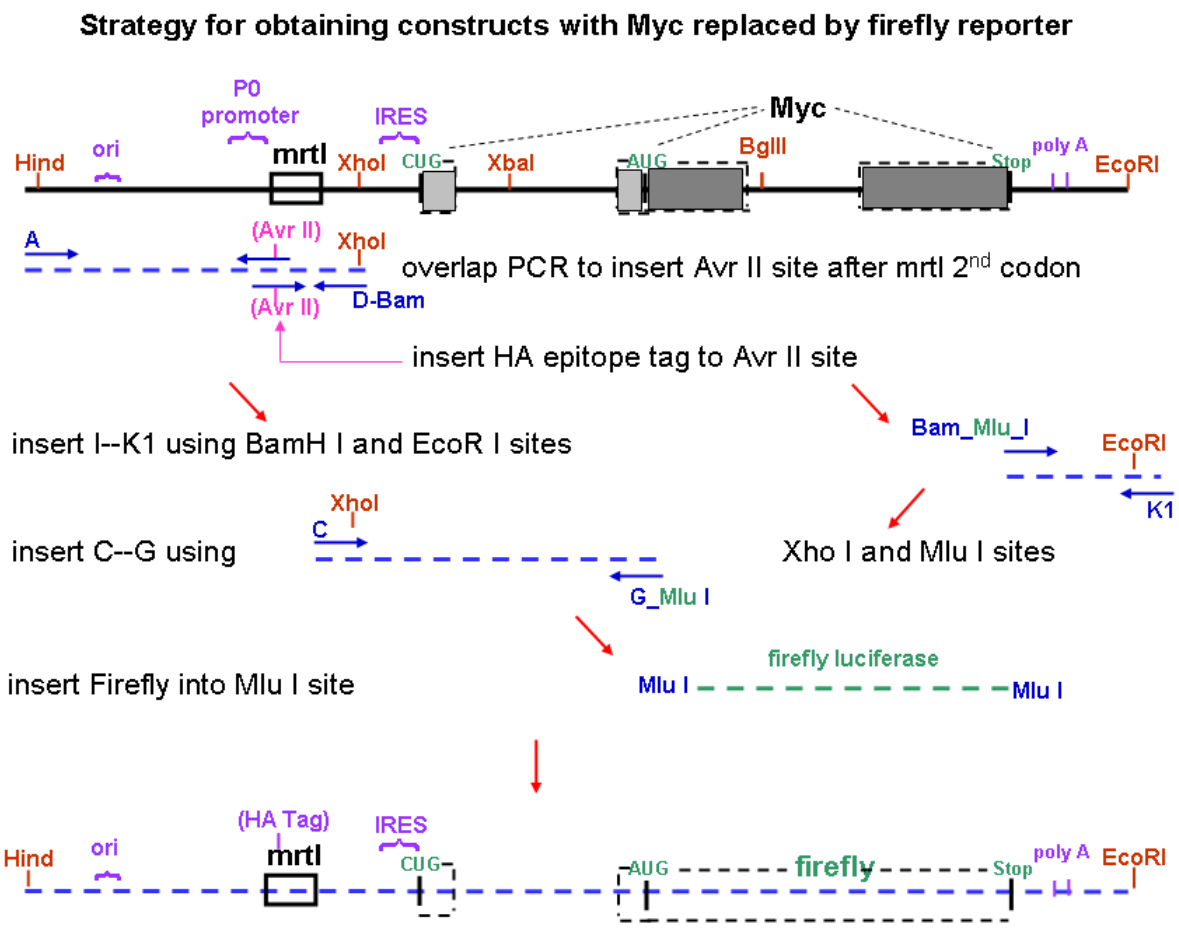


**Figure 1. Schematic depiction of the strategies used to develop two distinct series of Myc / mrtl expression / reporter constructs.** The thick black line represents the genomic DNA of the human c-*myc* locus (template). The mrtl (single exon) and Myc (three exons) coding sequences are represented by clear (mrtl) or shaded (Myc) rectangles respectively. The lighter shading represents the sequence unique to the p67 isoform of Myc (Myc1). The positions of the CTG (CUG) and ATG (AUG) initiation codons for p67 (Myc1) and p64 (Myc2) respectively are indicated as well. Key regulatory features are indicated in purple text: ori = eukaryotic origin of replication naturally occurring upstream of the mrtl coding sequence; P0 promoter driving expression of the Myc P0 transcript which is naturally tricistronic, including the coding sequences for mrtl, MycHex1, and Myc; IRES = internal ribosome entry site, an extremely important regulatory feature that controls the translational efficiency of Myc, and is likely influenced by mrtl; poly A = pair of natural polyadenylation signals present in the 3'-untranslated region of the Myc mRNA. Key restriction sites utilized in cloning strategy are indicated in red text. Blue dashed lines represent PCR products amplified from genomic DNA. Short blue arrows represent the PCR primers specifically designed to amplify individual segments of the Myc / mrtl locus. The PCR primers are given alphabetical designations which correspond roughly to their relative positions (upstream to downstream) on the Myc / mrtl locus sequence. The Avr II site in parentheses was incorporated in the midst of the A--D fragment by an overlap PCR strategy (see text). The BamH I, Nco I, and Mlu I sites were incorporated by inclusion within the 5'-tails of appropriate primers as indicated. Note that the order in which the individual segments were to be cloned was selected based on

anticipated cloning efficiency and incorporation of restriction sites into primer 5'-extensions rather than proceeding in an upstream to downstream direction. Also note that, with the exception of the Avr II, Nco I, and Mlu I sites, which were deliberately incorporated to facilitate insertion of the HA epitope tags and firefly coding sequence respectively, the remainder of the ~8.1 kb Myc / mrtl sequence is ultimately regenerated in a seamless manner with no gaps or foreign sequence inserted. **Scheme A** above depicts the strategy for obtaining constructs with epitope tagged mrtl and Myc. **Scheme B** below depicts the strategy for obtaining constructs in which the Myc coding sequence is precisely substituted for by the firefly luciferase coding sequence (while retaining all surrounding Myc regulatory sequences, including initiation codon (Kozak consensus), and stop codon).

The natural regulatory features positioned within this 8.1 kb region of the Myc / mrtl locus include: (1) the natural eukaryotic origin of replication positioned upstream of the Myc and mrtl coding sequences; (2) the native c-*myc* P0 promoter driving expression of the mRNA encoding both mrtl and Myc; (3) the mrtl coding sequence, including the Kozak sequence context surrounding the initiation codon; (4) the 5'-untranslated region including the c-*myc* internal ribosome entry site (IRES) positioned between the mrtl and Myc coding sequences; (5) the c-*myc* P1 and P2 promoters potentially driving expression of Myc independently (or at least in *trans*) relative to mrtl; (6) the Myc coding sequence including both natural Myc initiation codons (CUG and AUG) in their native orientations; (7) Myc introns 1 and 2; as well as (8) the native Myc stop codon, 3'-UTR, and natural polyA sites.

We had successfully amplified and subcloned the majority of the relevant sequence of the human c-*myc* locus into the pSTblue1 shuttle vector, however, the 3'-terminal region of this sequence (F6 -- K1) had proven to be more problematic. We found that by subdividing this region into two segments (F6--I and I--K1), amplification and cloning could be accomplished in a more efficient manner. Cloning of the F6--I segment had been reported in the previous Progress Report, thus the only remaining segment yet to be subcloned was the I---K1 segment (nucleotides 7213-8165 (with EcoRI site at 8083)). A new forward_I primer was designed to be compatible with the K1 primer:

Forward I = GTAAGGAAAAGTAAGGAAAACGATTC (26-mer)

The I--K1 sequence (952 bp) was successfully amplified from genomic DNA and subcloned into pSTblue1 (**Figure 2**).

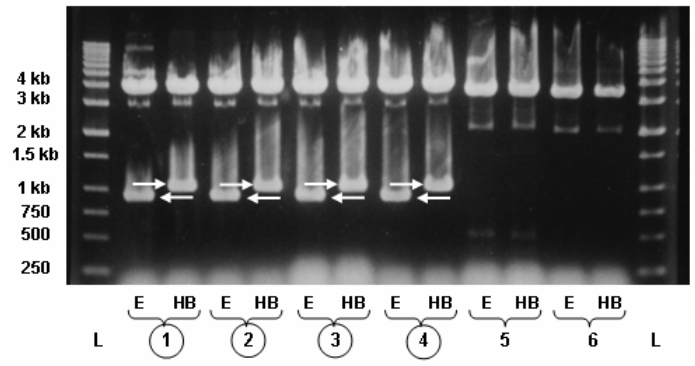


**Figure 2.** Successful subcloning of the I--K1 segment of the Myc locus into the pSTblue1 shuttle vector. Digestion with EcoRI alone (E) (cleaves both outside and within the insert) is expected to yield

a fragment of 870 bp, along with the 3.8 kb band representing the remainder of the plasmid. Digestion with Hind III plus BamH I (HB) is expected to excise the 952 bp insert. Clones 1-4 are positive.

The successful subcloning of the I--K1 fragment completed capture of the full extent of the Myc/mrtl locus sequence (8.1 kb in total) into the shuttle vector. Now attention was directed toward assembling these fragments into the destination vector, along with specific modifications necessary for the planned experiments. Our intention was to assemble the native Myc / mrtl sequence seamlessly into the destination vector in a manner which did not introduce any extraneous restriction sites or foreign sequences. The three exceptions to this were: (a) addition of an epitope tag to the N-terminus of the mrtl coding sequence; (b) addition of an epitope tag to the C-terminus of the Myc coding sequence; and (c) complete and precise replacement of the Myc coding sequence with the firefly luciferase coding sequence in one series of plasmids. In order to accomplish this seamless re-assembly, a series of overlapping fragments and naturally-occurring restriction sites were utilized, as described below.

We came to the conclusion that the epitope tags were important enough to justify inserting unique restriction sites into the native sequence. This would facilitate insertion of the tag (as a double stranded oligonucleotide), and also optional excision of either tag as needed to benefit particular experimental objectives (i.e. modular design). Also, we planned to insert a unique restriction site to facilitate cloning of the firefly luciferase coding sequence in place of Myc.

Therefore it was essential to select unique restriction sites, not already present within the destination vector (pGEM3Z), or anywhere else within the Myc / mrtl locus or firefly coding sequence. The following restriction sites were selected:

Avr II CCTAGG will add proline and arginine - select for insertion of HA tag to N-terminus of mrtl.

Nco I CCATGG will add proline and tryptophan, also potential additional start codon (out of frame) - select for Myc HA tag, positioned at C-terminus, where potential start codon will not interfere or compete with translation of the Myc coding sequence.

Mlu I ACGCGT will add threonine and arginine - select for insertion of firefly coding sequence.

All three of these enzymes cleave supercoiled DNA efficiently (facilitates single enzyme cloning). Since Avr II and Mlu I both cleave pSTblue1 (within multiple cloning region), it would not be feasible to insert the HA tag to mrtl nor incorporate the firefly coding sequence within the pSTblue1 (shuttle vector) context. Therefore, we concluded that it would be best to insert these into the pGEM3Z (destination vector) context directly, after all other genomic segments were in place.

Our initial strategy for incorporating these unique restriction sites into the native Myc / mrtl sequence involved use of a two-stage overlap PCR protocol. To make this possible, three new pairs of "internal" primers were designed, each of which contain: (a) hybridization segment; (b) restriction site; and (c) overlap with adjacent segment. The internal primers would be used in combination with the existing ("outer") primers which had already been used for initial PCR capture of each segment from genomic DNA.

outer internal / internal outer
A -- Breverse / B -- D for insertion of HA tag to N-terminus of mrtl coding sequence
F6 -- I / Iforward -- K1 for insertion of HA tag to C-terminus of Myc coding sequence
C -- G / Iforward) -- K1 for insertion of firefly cds to replace Myc coding sequence.

B_ReverseTail-2 = TAGAATGATTAAAATAACCCAGCA CCTAGG ACGCATTGCCACGTATACT (49-mer) includes Avr II site as position for insertion of HA tag to the N-terminus of mrtl. CAT represents mrtl initiation codon (in reverse orientation).

Myc_I_ReverseTag = GAATCGTTTTCCTTACTTTTCCTTA CCATGG CGCACAAGAGTTCCGTAGCTGTTC (55-mer) includes Nco I site for insertion of HA tag to the C-terminus of Myc, 5' portion overlaps Iforward--K1 including Myc stop codon and region beyond, 3'-portion hybridizes to I_reverse region near C-terminus of Myc coding sequence..

G--ReverseTail2 = GAATCGTTTTCCTTACTTTTCCTTA C ACGCGT TGGCATCGTCGCGGGAGGCT (52-mr) includes Mlu I site for insertion of firefly sequence in place of Myc coding sequence, 5' portion overlaps Iforward--K1 including Myc stop codon, 3' portion overlaps Myc first and second codons and upstream sequence (in reverse orientation).

Importantly, the primers were designed so as to maintain reading frame whether the epitope tag is in place or has been excised. Short versions of each of these multidomain primers, in which the extent of non-hybridizing 5'-tail was limited, were designed to be used for the initial rounds of PCR.

short-B--Reverse = TAGGACGCATTGCCACGTATACT

short-MycReverse = ATGGCGCACAAGAGTTCCGTAGCTGTTC

short-GReverse = GCGTTGGCATCGTCGCGGGAGGCT

We determined that a BamH I site could serve as temporary splicing site, which could be excised later to result in seamless regeneration precisely of the natural sequence with absolutely no extraneous base-pairs (except for the deliberately integrated HA-tags, firefly luciferase, and their associated restriction sites). For this purpose, additional versions of established primers were designed in which the BamH I site was incorporated as appropriate to the 5'-extension of the primer:

D_Bam = TAT GGATCC T CTGGAATTACTACAGCGAGTTAGAT

F6_Bam = TAT GGATCC T CTGGAGATGGTGACCGAGCTG

C_Bam = TAT GGATCC TGAGAGGGAGCAAAAGAAAATGGTA

The firefly luciferase (luc-plus) coding sequence was amplified from the second codon through the penultimate codon. This would allow us to retain the natural Myc initiation codon, including surrounding Kozak consensus sequence, and the Myc stop codon within its native sequence context.

firefly forward primer: ACTACGCGTGAAGACGCCAAAAACATAAAGAA

firefly reverse primer: CTGACGCGTTCCACGGCGATCTTTCCGCCCTT

The overlap PCR protocol which we developed for these experiments takes place in two distinct stages which are then ultimately combined into a single reaction. The protocol uses a low concentration of internal primers and a limited number of cycles (10) to begin amplifying the two half-products in two separate reaction tubes. These two half-reactions are then combined into a single tube and 2 cycles performed to generate the full-length product by hybridization and extension of overlapping segments. Finally, the concentration of the outer primers is supplemented (now in excess of the internal primers) and 25 additional cycles performed to facilitate high yield amplification of the full-length overlap product. The initiation of the PCR amplification reaction (addition of the thermostable polymerase), as well as combination of two half-reactions, and supplementation of external primers, were are each performed at elevated temperature (e.g. hot-start, hot-combination of half-reactions, and hot-supplementation of external primers), to limit non-specific hybridization and enhance specificity. As appropriate, a longer extension time is used for the final 25 cycles (amplification of the full-length product) relative to the initial half-reactions.

The product is analyzed by digestion with the restriction enzyme whose recognition sequence was intended to be incorporated into the overlap segment. The key outcome is to gauge whether at least 25-50% of products are cleavable (i.e. that the product is derived from the overlap reaction rather than amplification from the original template). Critical to the success of this strategy are relatively low input of original plasmid template and low concentration of internal primers. Limiting these components is necessary so that generation of full-length overlap product will compete favorably with direct amplification from the original plasmid template, as well as cumulative generation of products of the two half-reactions.

The first overlap PCR used primer A combined with B_reverseTail2 in one half-reaction and primers B and D_Bam in the other. The two half-reactions were combined and the outer primers A and D_Bam supplemented. The desired full-length product (**Figure 3**) would cover the full A--D segment but with incorporation of an Avr II site at the position of the mrtl third codon.

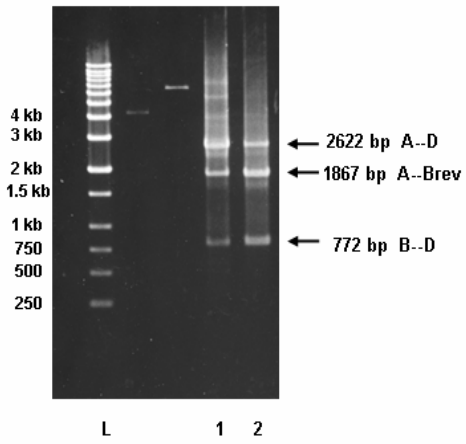

**Figure 3. Overlap PCR of the Myc / mrtl A--D segment, introducing unique Avr II site after the mrtl second codon.** Two separate PCR reactions were initiated, one utilizing primers A and BreverseTail2 and the other utilizing primers B and D. The 5'-extension of BreverseTail2 incorporated both an Avr II site as well as a segment overlapping forward primer B. Following 10 cycles to initiate amplification in each of these half-reactions, the two reactions were combined and two additional cycles performed to allow for overlap hybridization and extension. Then external primers A and D_Bam were supplemented, and an additional 25 cycles of amplification performed. Shown in lane 1 is an aliquot of the final product. Products of each of the two half-reactions (A--Breverse = 1867 bp; B--D = 772 bp) are visible, as well as the full-length product A--D (2622 bp). Lane 2 has been digested with the Avr II restriction enzyme, which would cleave the full-length product generated by successful overlap PCR, but would not cleave any full-length product generated from the original template. Reciprocal changes in intensities of the bands are observed upon digestion with Avr II: a decrease in intensity of full-length product is accompanied by an increase in intensity of the two half-products.

We found that digestion of the overlap PCR product directly without purification (betaine and DMSO cosolvents still present) is possible at least for some enzymes (Avr II, Mlu I, Hind III), though associated with star activity for others (BamH I).

Successful cloning of the A--D overlap segment into the destination vector (pGEM3Z) was accomplished using the Hind III (position 1 within Myc / mrtl locus sequence) and BamH I (synthetically incorporated into D primer tail) sites (**Figure 4**). We found that cloning efficiency of these relatively large inserts could be increased by decreasing the plasmid input into the ligation reaction, thus effectively increasing the insert to vector ratio.

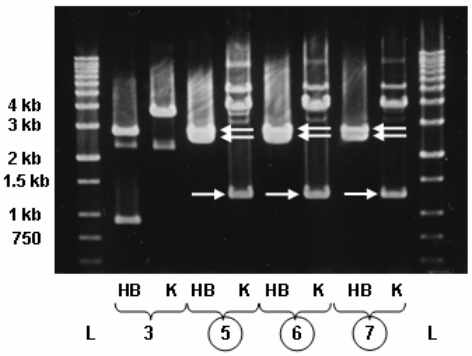


**Figure 4. Cloning of the A--D overlap segment with Avr II site into the destination vector.** To assess potential recombinant clones, Hind III - BamH I (HB) double digestion was used. This would be expected to excise the insert = 2.5 kb, leaving the remainder of the vector = 2.7 kb. Digestion with Kpn I alone (K), which recognizes a site just outside of the insert, along with one site in the middle of insert, was expected to yield 1.2 kb and 4.0 kb fragments. Clones 5, 6, and 7 (shown), as well as 9, 10, 11, and 12 (not shown) are positive. An Avr II - Hind III double digest, yielding 1.7 and 3.5 kb bands (not shown, correct in all 7 positive clones) was used to confirm these constructs.

The overlap PCR of C--K1 (3,404 bp) with insertion of a MluI site for firefly to replace Myc also was successful (**Figure 5**). The two half-reactions were C_Bam -- G_reverseTail2 (2452 bp, ends at Myc initiation codon) and forward-I -- K1 (952 bp, begins at Myc termination codon).

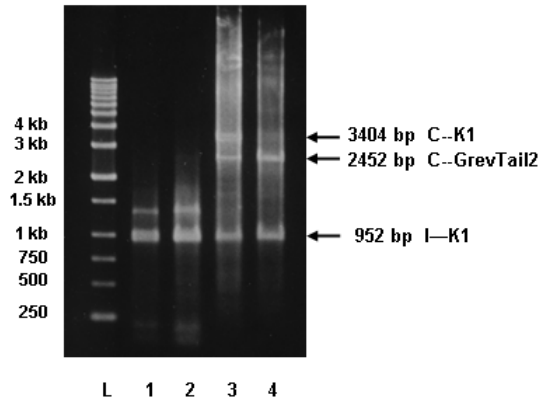


**Figure 5. Successful overlap PCR of the C--K1 segment with insertion of MluI site after the Myc initiation codon.** The half-reaction utilizing primers C_Bam and GreverseTail2 yields a product of 2452 bp, while the half-reaction utilizing primers forward_I and K1 yields a product of 952 bp. The full-length product generated by overlap hybridization and amplification using C_Bam and K1 is 3404 bp (lane 3). There is good evidence for digestion with Mlu I (even in the presence of PCR buffer, lane 4), leading to near complete disappearance of the full-length product and a reciprocal increase in intensity of the two half-reaction products. This result is indicative of the desired full-length overlap product containing the synthetically inserted Mlu I site. The overlap PCR F6--I / I--K1 reaction also appeared to have been successful, though there was relatively low quantitative yield of the full-length product (data not shown).

Our next objective was to clone the HA epitope tag into the Avr II site within the A--D segment. This would enable ectopically-produced mrtl to be detected specifically using an anti-HA antibody. The small HA sequence could be cloned as a double stranded synthetic oligonucleotides with Avr II-compatible cohesive ends built into each side, as follows:

mrtl_HA_top: CTAGGTACCCATACGATGTTCCAGATTACGCTC

mrtl_HA_bottom: CTAGGAGCGTAATCTGGAACATCGTATGGGTAC

The two oligonucleotides were combined under relatively dilute conditions, heated to ensure denaturation, cooled slowly to allow for hybridization to occur, and then added to the ligation reaction along with Avr II-digested pGEM_A--D.

This was a non-directional cloning event, with a very small insert, thus it could potentially be very difficult to discern either the presence of the insert as well as its orientation. However, we noted that with this particular sequence, incorporation of the HA tag in the correct orientation would generate a new Kpn I site near the 5' end of the insert, and this greatly facilitated analysis of the clones (**Figure 6**).

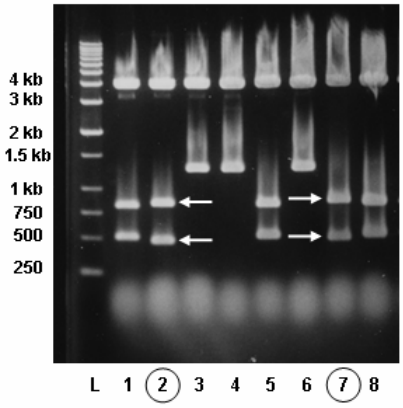


**Figure 6. Cloning of the HA epitope sequence into the A--D segment (at the mrtl N-terminus) using the Avr II site.** The sequence encoding the HA epitope (9 amino acids) was regenerated by hybridizing two synthetic oligonucleotides, and this sequence was ligated into pGEM3Z_A--D following its digestion with Avr II. The ligation event would generate a new Kpn I site asymmetrically positioned in relation to the insert. Another Kpn I site is already contained within the A--D segment at 1271 (for reference, the Avr II insertion point after the mrtl second codon is at 1737). Therefore, the status of the clones could be distinguished (by Kpn I digest alone) as follows: No insert: 1,240 and 4,014 bp bands. Insert in desired orientation: 466, 797, 4014 bp bands. Insert in opposite orientation: 491, 772, and 4014 bp bands. Clones 2 and 7 are positive. Clones 1, 5, and 8 contain the insert in the opposite orientation.

It was very important to confirm this important clone, which would serve as the source for generation of the remainder of the constructs, by direct sequence analysis (**Figures 7-8**). Note that reading frame is precisely maintained, and that no insertions, deletions, or other extraneous sequence are introduced.

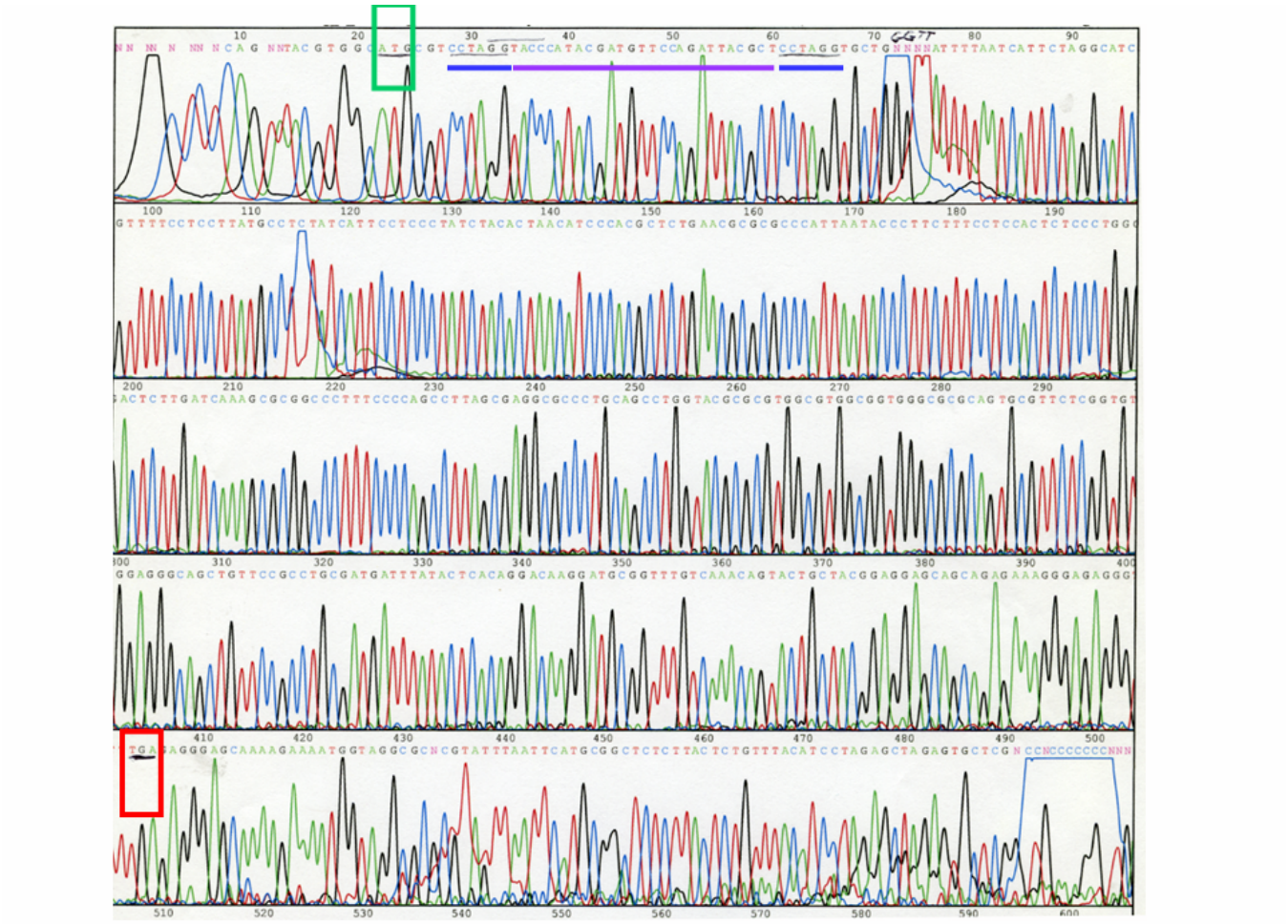

**Figure 7.** Direct sequence analysis of pGEM3Z_A--D_mrtlTag (forward direction). The position of the mrtl initiation codon is marked by green rectangle. The mrtl stop codon is marked by red rectangle. Positions of the Avr II sites are indicated by thick blue lines, while the inserted HA epitope sequence is marked by a thick purple line.

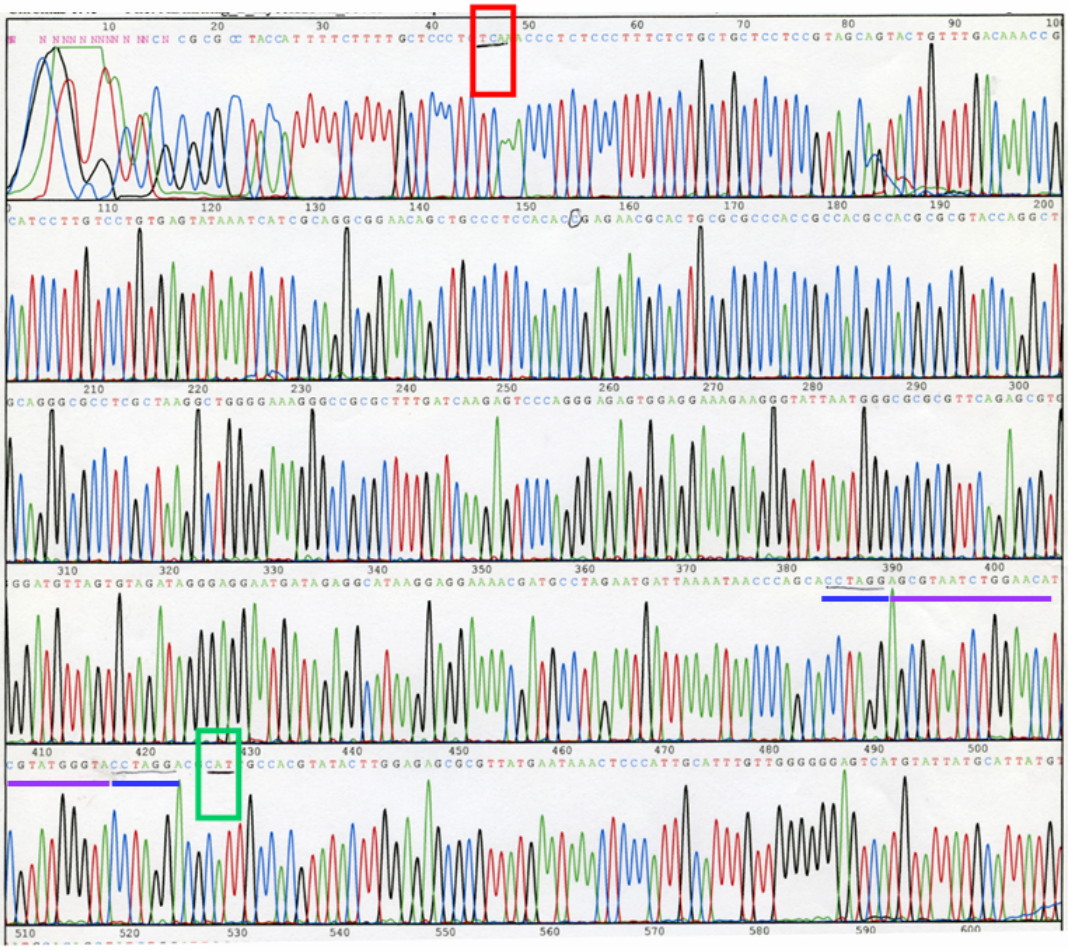

**Figure 8.** Direct sequence analysis of pGEM3Z_A--D_mrtlTag (reverse direction). The position of the mrtl initiation codon is marked by green rectangle. The mrtl stop codon is marked by red rectangle. Positions of the Avr II sites are indicated by thick blue lines, while the inserted HA epitope sequence is marked by a thick purple line.

Having confirmed the status of this construct, it was worthwhile to test this construct by transient transfection into human breast tumor cells. Our plan was to use an antibody to the HA tag to specifically detect ectopically produced (tagged) mrtl, and use mAb131 to measure total (endogenous plus ectopic) mrtl. By comparing intensity of the mAb131 band in transfected cells to that of untransfected cells, it should be possible to gauge the degree of ectopic mrtl expression relative to endogenous mrtl. Any changes in Myc levels induced by ectopic mrtl expression (in *trans* with this particular construct) would be sought. Cells transiently transfected with a standard EGFP expression vector (CMV promoter, no eukaryotic origin of replication) would be used as a control.

Cells were transfected using FuGene6, which does not require serum deprivation (i.e. OptiMEM). This is important because Myc regulation is influenced by changes in serum concentration. Following transfection, cells were propagated continuously and aliquots harvested at different time points for preparation of whole cell protein extracts which could be used to assess Myc and mrtl levels by western analysis. We anticipated that the naturally-occurring eukaryotic origin of replication (3-4) contained

within the A--D segment upstream of the mrtl coding sequence might enable the A--Dmrtl_tag plasmid to persist within transfected cells and ectopic mrtl to be expressed indefinitely (3) (4), without selection or reliance on rare genomic integration events. In contrast, we expected EGFP protein levels to dissipate rapidly after several days in culture, as is typical of transient transfection. Two human breast tumor cell lines were transfected: T47D (ER-positive) and MDA-MB-231 (ER-negative). This was important because major distinctions in Myc regulation are known to exist between ER-positive and ER-negative breast cells (5).

Endogenous mrtl was readily detectable by mAb131 in each of the cell samples (**Figure 9**).

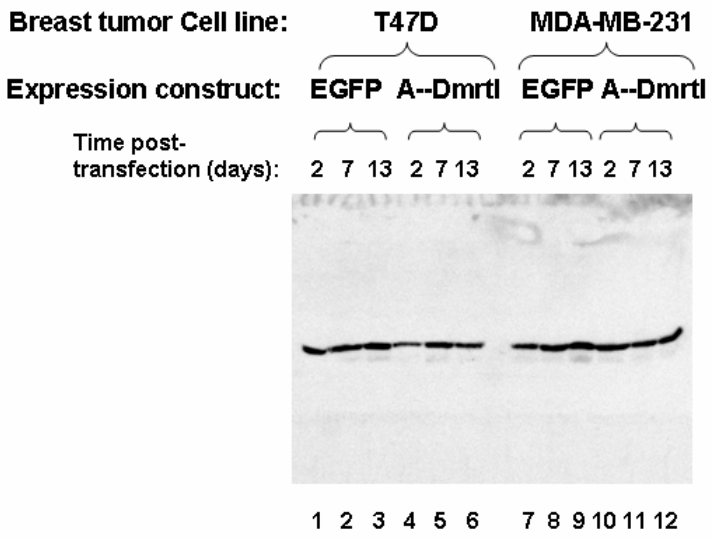


**Figure 9.** T47D (ER-positive) or MDA-MB-231 (ER-negative) human breast tumor cells were transfected (FuGene6) with pGEM3Z_A--Dmrtl_tag (lanes 4-6 and 10-12) or a standard expression plasmid for EGFP (lanes 1-3, 7-9). Cells were propagated continuously following transfection. At various time points (2, 7, or 13 days post-transfection), aliquots of cells were subjected to whole cell extraction and equivalent aliquots of protein loaded on a 17.5% SDS/PAGE. Following transfer to nitrocellulose, mrtl was detected using mAb 131 (mouse monoclonal), HRPO-conjugated goat-anti-mouse secondary antibody, and standard ECL reagents.

However, a clear increase in total mrtl in cells transfected with the A--Dmrtl_tag construct was not observed, and evidence of specific reactivity to the HA tag (indicative of ectopically synthesized mrtl) was not observed at any time point (data not shown). This negative result could be due to a technical problem with the anti-HA reagent, low transfection efficiency, low ectopic expression of mrtl from the native P0 promoter, or incomplete post-translational modification of the ectopically-synthesized mrtl (as is the case for ectopic mrtl synthesized under control of the CMV promoter) and consequently limited recognition by mAb131.

The native P0 promoter was deliberately selected for these applications in attempt to avoid problems associated with supraphysiological overexpression from a strong constitutively active promoter. The construct tested in this experiment represents an intermediate which lacks the Myc coding sequences as well as the 3'-UTR (including polyadenylation sites). The lack of 3'-UTR (6) and polyadenylation signal within this particular construct could further contribute to relatively low expression or failure to

express ectopic mrtl. Furthermore, although great care has been taken to include as much of the natural Myc locus sequence context as possible, it is yet conceivable that additional long-distance interactions with other regulatory sequences that are not included in the expression construct may be required for effective expression. It is also possible that ectopic expression of mrtl could impact cell cycle progression if, as we have hypothesized, mrtl exerts a potent regulatory effect on Myc. If cells expressing mrtl fail to divide or divide infrequently, then ectopically-produced mrtl from those cells may be difficult to detect, and would become progressively diminished by dilution due to continued propagation of the untransfected cells. Additional experiments planned will utilize immunofluorescence in attempt to discern the expression of ectopic mrtl.

We planned to utilize the overlap PCR strategy to incorporate each of the three unique extrinsic restriction sites which would then be used to insert the HA epitope tags and the firefly coding sequence. However, although the A--D segment with Avr II site inserted by overlap PCR was successfully cloned, and the C--K1 and F6--K1 overlap PCR reactions themselves were also successful, we were not able to successfully clone the C--K1 and F6--K1 overlap PCR products into the destination vector.

At least two factors likely contributed to these difficulties: the relatively low yield of the full-length product and the relatively large size of the inserts (3.3 kb each). Therefore, we tried repeating the overlap PCR in attempt to increase yield. We determined that intermediate use of the "short" primers with limited 5'-extensions was not necessary. We tested whether it would be beneficial to perform 20 cycles of amplification of the half-reactions prior to combining for overlap and generation of the full-length product, but found that this was associated with a lower yield. Variations in the cosolvents betaine and DMSO were tested as an alternative to modifications in Tm to achieve optimal yield and specificity of PCR product. We found this was a very beneficial strategy which allows multiple such modifications to be tested in parallel (in the same block). We found that a decrease in betaine from 1M to 0.5M was associated with higher degree of specificity (higher stringency), yet low yield. A decrease in DMSO from 10% to 5% was associated with much higher yield (lower stringency). Combining 0.5M betaine with 5% DMSO (both parameters decreased from standard conditions) was associated with lower yield and no improvement in specificity. However, we found that combining the standard 1M betaine with a modest decrease in DMSO to 7.5% was associated with a substantial increase in yield and simultaneously an increase in specificity of the desired product.

For the C--K1 overlap PCR reaction, a decrease in Ta combined with a decrease in DMSO, both intended to relax stringency and thereby boost efficiency of overlap PCR, clearly was beneficial. We also tested an alternative strategy in which the concentrations of internal primers and plasmid template were decreased further, with goal of increasing specificity; however, this was not beneficial, indicating that limited efficiency of overlap PCR was more of a critical factor than was competition from half-reactions or full amplification from the original plasmid template.

As an alternative strategy, we elected to subclone the individual products of each of the half-reactions from the overlap PCR sequentially, essentially accomplishing the same objective but with smaller and higher quantity inserts. Additional primers were designed to facilitate this series of ligations:

H2-Bam = ACT GGATCC GAAGTGGATTGAGTTGTAAGATAAGC

Bam-Nco-I_forward = TCA GGATCC ATGG TAAGGAAAAGTAAGGAAAACGAATTC

I_reverse_Nco = GAT CCATGG CGCACAAGAGTTCCGTAGCTGTTC

Bam-Mlu-I_forward = CTA GGATCC AACGCGTGTAAGGAAAAGTAAGGAAAACGATTC

G_reverse-Mlu = GACACGCGTTGGCATCGTCGCGGGAGGCT

A series of new PCR reactions were accomplished to generate the individual products to be cloned:
C--H2_Bam (3.4 kb)
Bam-Nco_I_forward -- K1 (952 bp)
F6 -- I_reverse_Nco (2.4 kb)
Bam-Mlu_I_forward -- K1 (952 bp)
C -- G_reverse_Mlu (2.4 kb)

We proceeded to work toward further development of the two series of composite constructs in parallel: (i) those in which mrtl and Myc would both be tagged; (ii) those in which mrtl would be followed by firefly luciferase reporter precisely replacing the Myc coding sequence. For the Myc / mrtl series, the necessary steps could be outlined as follows:

(a) clone C--H2 into A--DmrtlTag using Xho I and BamH I sites - yielding A--H2

(b) insert I--K1 using BamH I and EcoR I sites - yielding A--H2_I--K1

(c) insert F6--I using Bgl II and Nco I sites - yielding full-length A--K1mrtlTag

(d) clone HA tag into Nco I site (at Myc C-terminus) - yielding A--K1mrtlTagMycTag

For the firefly reporter series, the necessary steps could be outlined as follows:

(e) clone I--K1 into A--DmrtlTag using BamH I and EcoR I sites - yielding A--D_I--K1

(f) insert C--G_Mlu using Xho I and Mlu I sites - yielding A--K1Mlu

(g) insert firefly luciferase coding sequence into Mlu I site - yielding A--K1mrtlTagFirefly

First the C--H2 segment was cloned into A--DmrtlTag (**Figure 10**).

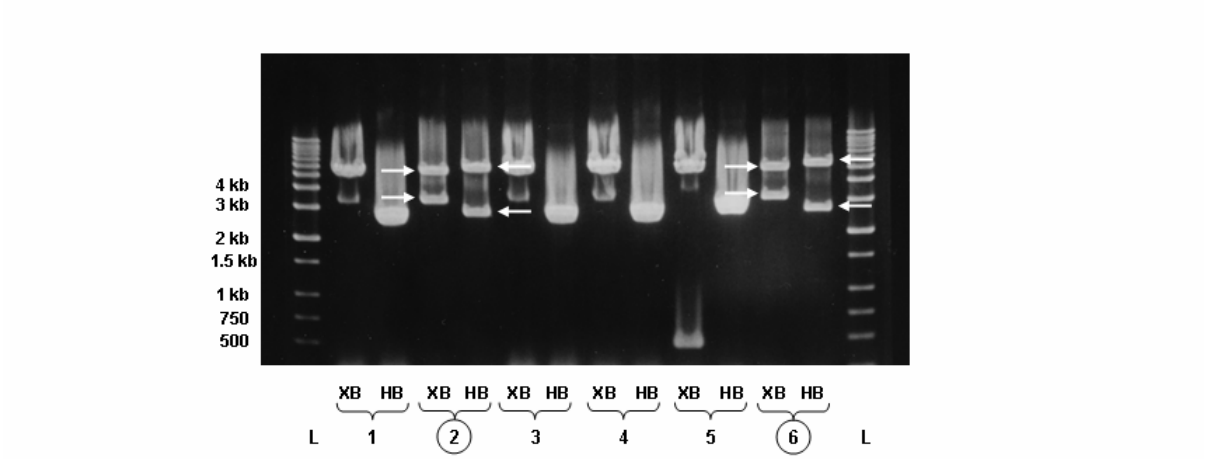


**Figure 10.** Successful cloning of the C--H2 segment into A--DmrtlTag. XhoI - BamH I double digestion (XB) excises the C--H2 insert (3.1 kb), leaving A--D and the remainder of plasmid (5.1 kb). Hind III - BamH I double digest (HB) excises the composite A--H2 insert (5.5 kb), leaving the plasmid backbone (2.7 kb). Clones 2 and 6 are positive.

At this point, the plasmid contains the composite A--H2 Myc / mrtl sequence, including the HA epitope tag at the mrtl N-terminus. This construct was then verified by sequencing, focusing in particular on the junctions between recombinant segments (**Figures 11-14**). Several primers were utilized: primers C and D surround the Xho I junction, F6 points toward the H2--Bam junction, while the M13 forward primer points toward the EcoR I (downstream) end of the Myc sequence.

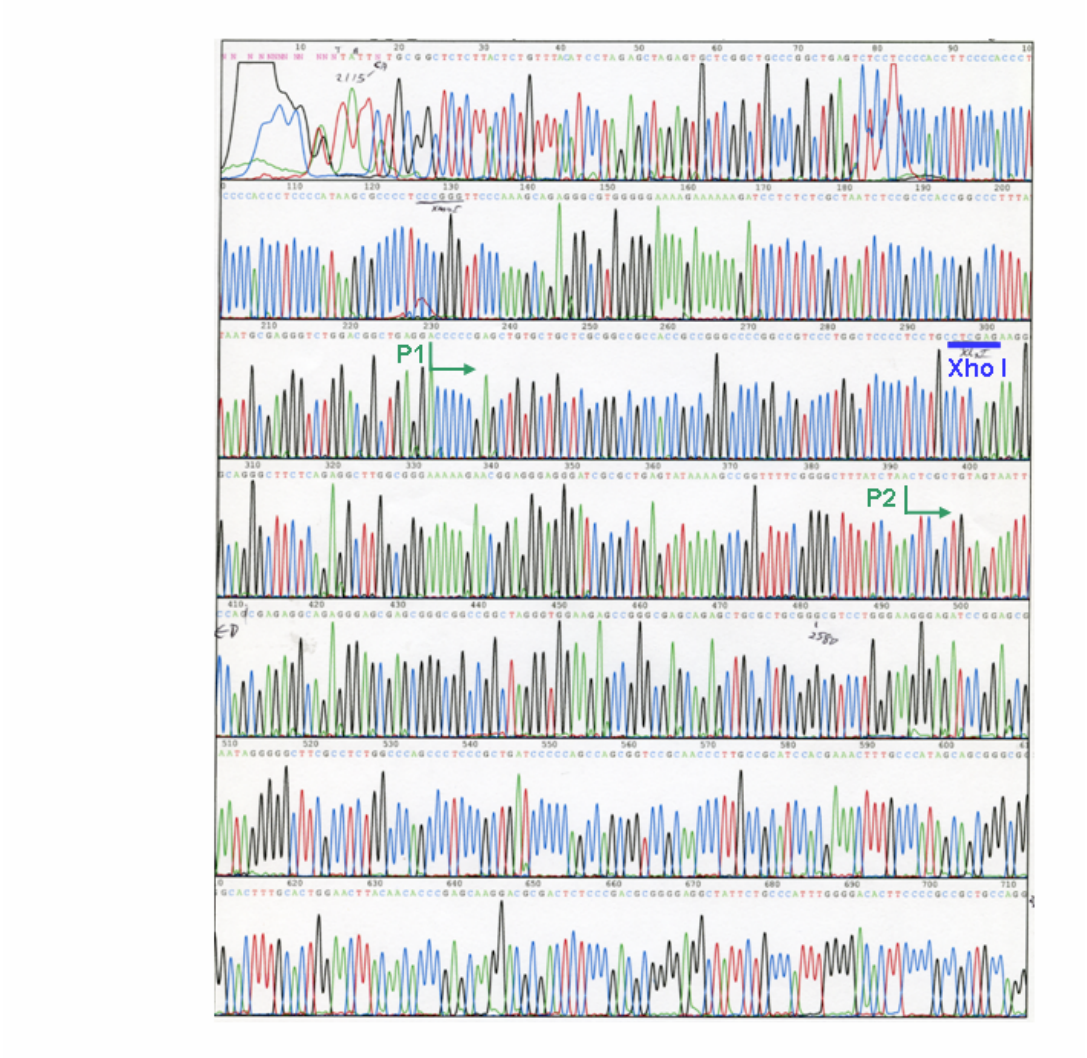


**Figure 11. Sequence analysis of composite A--H2 cloned sequence (forward direction)**. Positions of the Myc P1 and P2 transcription start sites are indicated (green arrows), as is the naturally-occurring Xho I site (blue bar), which was utilized for seamless integration of the C--H2 segment with the overlapping A--D segment.

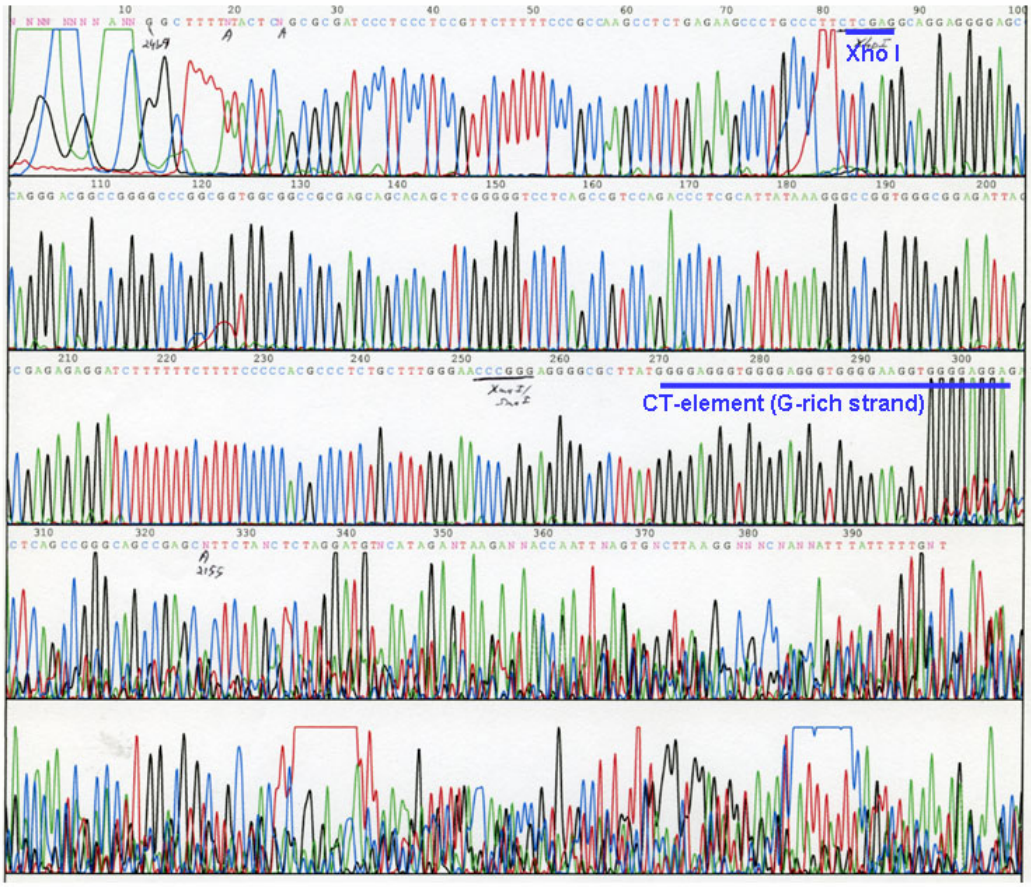


**Figure 12. Sequence analysis of composite A--H2 cloned sequence (reverse direction)**. Position of the naturally-occurring Xho I site (short blue bar), which was utilized for seamless integration of the C--H2 segment with the overlapping A--D segment, is indicated. Note that, as expected, the sequence becomes uninterpretable as the polymerase encounters the G-rich strand of the well-studied CT-element of the P1 promoter, which is prone to adopt highly stable secondary structures such as an intramolecular triplex.

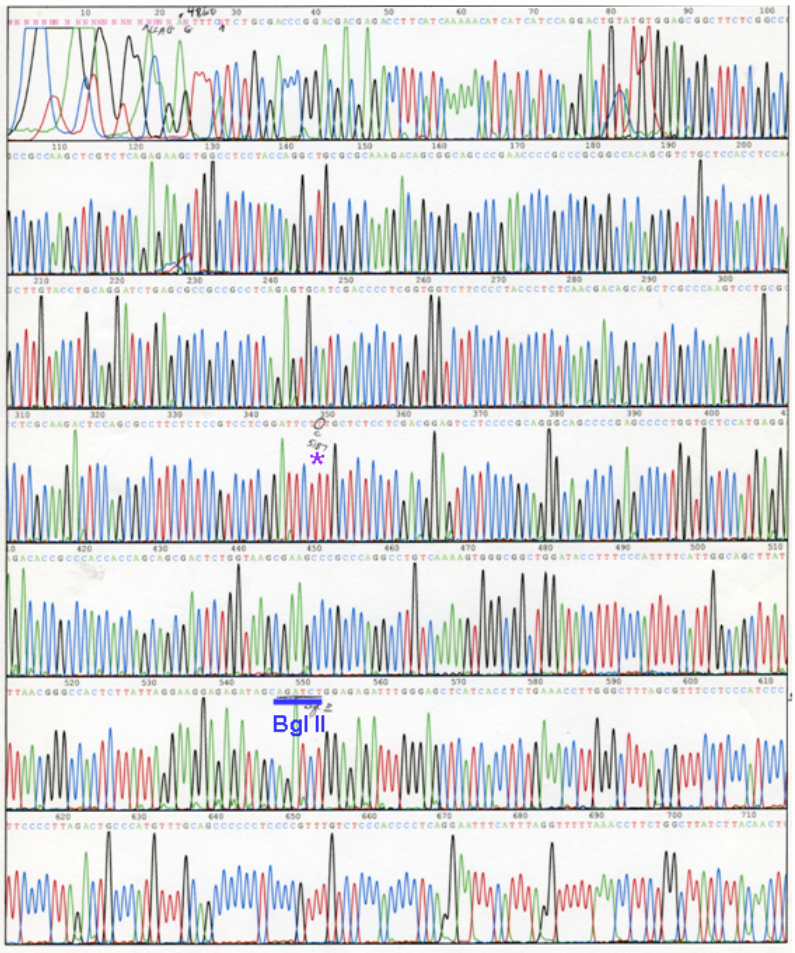


**Figure 13. Sequence analysis of composite A--H2 cloned sequence (forward direction)**. Positions of the naturally-occurring Bgl II site (blue bar) as well as single nucleotide polymorphism (C to T) at 5187 (asterisk), are indicated.

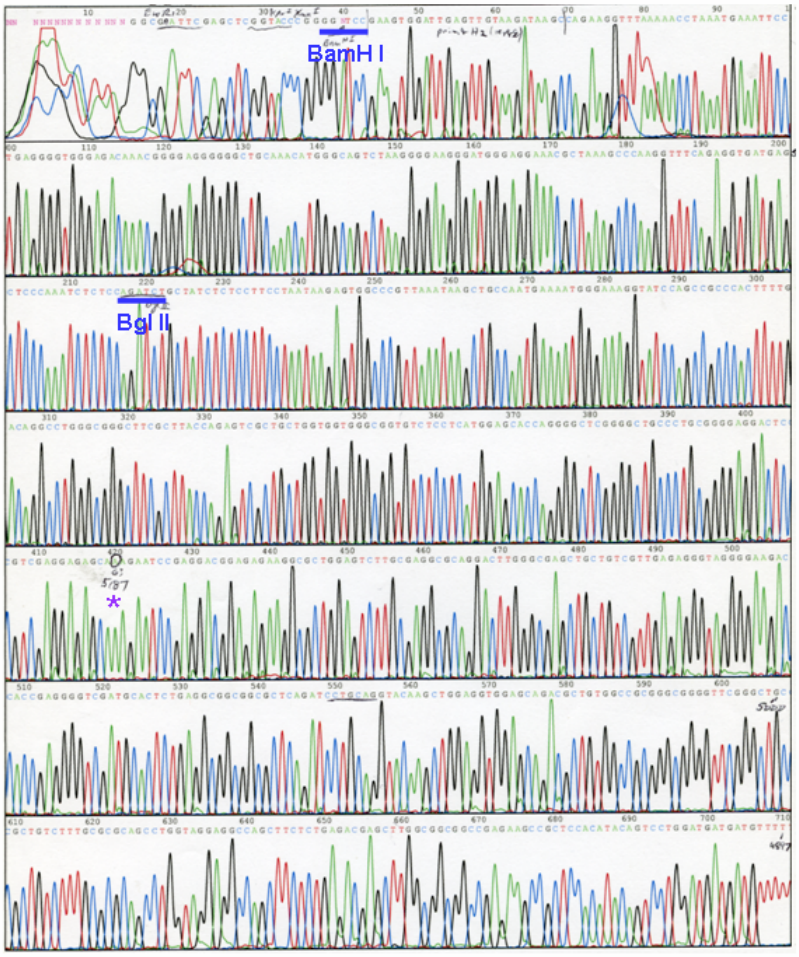


**Figure 14. Sequence analysis of composite A--H2 cloned sequence (reverse direction)**. Positions of the naturally-occurring Bgl II site (blue bar), the BamH I site located just outside the H2 primer within the vector cloning region, as well as single nucleotide polymorphism (G to A) at 5187 (asterisk), are indicated.

All junctions were verified. No insertions or deletions were detected. However, possible single nucleotide polymorphisms were identified:

**5187 C to T** (confirmed in both directions) represents first position in codon 223, synonymous (leucine) CTG to TTG

**4854 A to G** represents first position codon 112, non-synonymous AAC to GAC = Asn to Asp

**4686 C to T** represents first position codon 56, synonymous CTG to TTG (leucine)

The next objective was to clone Bam-Nco_I--K1 in to A--H2 using BamH I and EcoR I sites (**Figure 15**).

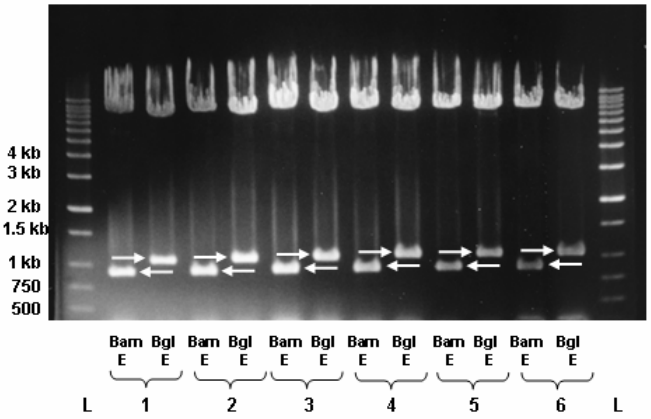


**Figure 15.** Cloning of I--K1 into A--H2. Digestion with BamH I and EcoR I (BamE) would excise the new insert of 870 bp, leaving the remainder of the plasmid at 8306 bp. Digestion with Bgl II and EcoR I (BglE) is expected to yield 1043 bp plus 8133 bp fragments. 11 out of 12 clones (including all shown above) were positive.

Next, for the Firefly series of constructs, the I--K1 segment was cloned into A--DmrtlTag using the BamH I and EcoR I sites (**Figure 16**).

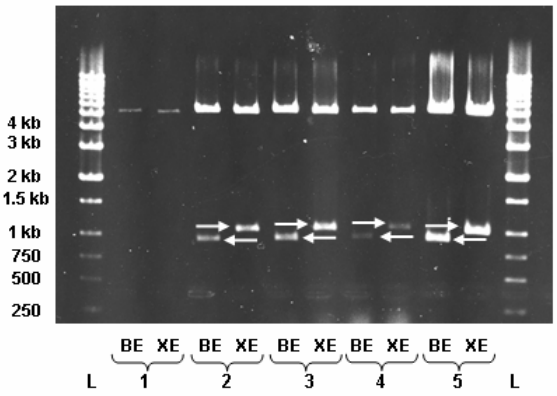


**Figure 16.** Successful cloning of the I--K1 segment into A--DmrtlTag. BamH I - EcoR I (BE) double digestion yields an 870 bp fragment plus the remainder of the construct (~5.2 kb). Digestion with XhoI - EcoR I (XE) yields a 982 bp fragment plus the remainder of construct (~5.2 kb). Clones 2, 3, 4, and 5 are positive.

The next objective was to clone the C--G-Mlu segment into the composite construct using the Xho I and Mlu I sites (**Figure 17**). This would complete the Myc / mrtl sequence (except for the Myc coding region itself) and be ready for insertion of the firefly reporter sequence.

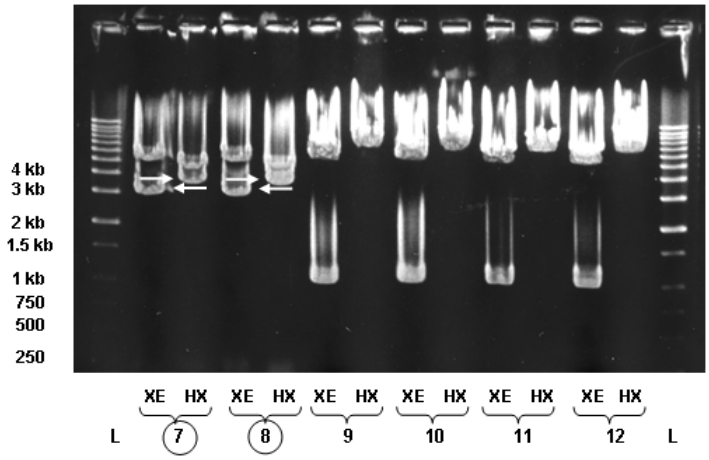


**Figure 17.** Cloning of the C--G segment into the A--D_I--K1 composite vector. Digestion with Xho I and EcoR I (XE) is expected to yield a 2998 bp fragment plus the 5.1 kb remainder of the construct. Digestion with Hind III and Xba I (HX) is expected to yield a 3510 bp fragment plus 4.6 kb remainder of the construct. Clones 7 and 8 are positive.

**Task 2: Examination of mrtl in human breast tumor specimens and non-malignant breast tissues, and correlation of these findings with Myc status and clinical parameters to obtain evidence for the possible involvement of mrtl in human breast cancer pathogenesis.**

We have made significant progress in the acquisition of additional human breast tumor specimens, including metastatic lesions, adjacent uninvolved tissues, as well as normal breast specimens as control tissues. We have successfully acquired an additional 8 primary invasive breast carcinoma specimens, 1 metastatic lesion of breast tumor origin, 3 adjacent uninvolved tissues from breast cancer patients, and 4 normal breast tissue specimens for use as controls (reaching a total of 51 breast specimens from 46 patients undergoing diagnostic / therapeutic surgical procedures). Included within this most recently acquired group are 5 specimens with no overt pathology but obtained from patients with strong family and/ or personal history of breast cancer and/or BRCA1 mutation (prophylactic surgery). Of the malignant specimens (primary breast tumors and metastases) obtained thus far, 13 are ER-positive and 9 are ER-negative.

Relevant details and descriptions of these specimens are provided below:

**Primary breast tumors:**

**29-10-03-A079d** - 58yowf, infiltrating ductal adenocarcinoma (primary), **ER/PR-positive, Her-2/neu-negative,** modified Bloom-Richardson **grade II**/III, maximum tumor dimension **3.0 cm, pT2; N1**; MX, (see **30-10-03-A080d** for lymph node metastasis of same patient).

**33-10-06-A054i** - 60 yowf, **invasive ductal adenocarcinoma** (primary), **s/p chemo**, **ER-positive, PR-negative, Her2-neu-positive**, **lobular features**, **21 cm**, modified Bloom-Richardson **grade III/III, ypT3; N2**. metastatic carcinoma involving **4/11 lymph nodes**, **extranodal extension**, treatment effect, (right side, lobular CIS, multifocal, areas of sclerosing adenosis); poorly demarcated extensive mass throughout breast, matted lymph nodes.

**39-10-07-A095g -** 58 yobf, invasive malignant **adenocarcinoma, lobular**, primary, **triple negative, s/p chemoRx**. **two foci**, largest **11.5 cm**, modified Bloom-Richardson **grade II**/III, **extensive lymphovascular invasion**, **6/13 lymph nodes** positive metastatic carcinoma, **extranodal extension, pT3; N2a**; MX, poorly defined firm nodular infiltrative mass.

**40-10-07-A170d -** 42 yowf, invasive **adenocarcinoma, ductal** (primary), **ER/PR-positive, Her2-negative**, **2.3 cm**, modified Bloom-Richardson **grade III**/III, **DCIS high nuclear grade**, cribriform and solid types, **pT2; N1. sentinel node metastatic carcinoma** 1.1 mm, **without extranodal extension** (total **1/3** nodes positive), gritty infiltrative mass.

**42-10-10-A177i -** 60 yowf, **invasive ductal adenocarcinoma** (primary), **triple negative**, **20.5 cm,** modified Bloom-Richardson **grade III**/III, extensive **necrosis, ulceration** of overlying skin, **perineural invasion, lymphovascular invasion, 1/14 lymph nodes** positive metastatic carcinoma with **extranodal extension**, 2.5 cm **pT4b / N1a**. **displaced nipple areolar complex**, ulceration 8.5 x 7.5 cm, extensive **necrotic** mass, **lymph nodes** grossly positive, **invades dermis**, glandular differentiation score 3; nuclear pleomorphism: score 3; mitotic count: score 3; overall grade 3. **no presurgical therapy**.

**45-11-02-A034l -** 43 yowf, invasive lobular **adenocarcinoma** (primary), **ER/PR-positive, Her2-negative.** fibrosis, **signet ring features,** modified Bloom-Richardson **grade II**/III, **10.5 cm**, **lymphovascular invasion, 6/6 axillary lymph nodes** positive metastatic carcinoma, **prominent mucin production**, 2.9 cm largest, **extracapsular extension, ypT3; N2a. s/p chemotherapy**. slight nipple retraction, markedly firm skin, thick fibrous rubbery to firm mass, fibrotic to gritty, **invades dermis** but no ulceration, **glandular/tubular differentiation = 3**; **nuclear pleomorphism = 3**; **mitotic count =1; grade 2**; **probable or definitive response to presurgical therapy in breast and lymph nodes.**

**46-11-03-A031d -** 61 yowf, invasive ductal **adenocarcinoma** (primary), **ER/PR-positive**, modified Bloom-Richardson **grade III**/III. **2.2 cm**, **no DCIS component**, **no lymphovascular invasion. 0/30 lymph nodes**. **multicentric, multifocal triple negative, s/p neoadjuvant therapy**. gritty lesion embedded within fibrous area, extensive necrosis within, three nodules. glandular/tubular differentiation = 3; nuclear pleomorphism = 3; mitotic count = 3. **pT2;** N0, (also see **47-11-03-A032d** for adjacent uninvolved tissue from same patient).

**48-11-04-A001g -** 52 yobf, invasive ductal **adenocarcinoma (**primary), **0/17 lymph nodes**. **4.8 cm,** modified Bloom-Richardson **grade III**/III. previous biopsy, microcalcifications in non-neoplastic breast ducts, fibrocystic changes consisting of stromal fibrosis, microcystic dilations, apocrine metaplasia, **cavitary lesion** 10.5 cm fluid-filled, solid papillary mass **4.8 cm**. glandular differentiation = 3, nuclear pleomorphism = 3, mitotic count =3; **no known presurgical therapy**, **no lymphovascular invasion, pT2; N0. triple negative.** (Also see 49-11-04-A002g for adjacent uninvolved tissue from same patient)

**Metastatic lesions of breast tumor origin:**

**30-10-03-A080d - (same patient as 29-10-03-A079d) -** infiltrating ductal adenocarcinoma, **metastatic to lymph node**, **ER/PR-positive, Her-2/neu-negative,** grossly positive for malignancy, 1.2 cm.

**Non-malignant reference tissues:** adjacent uninvolved breast or reference tissues from patients with breast tumors.

**32-10-05-A034e** - 45yowf, **lymph node, benign**, **s/p chemo**, **all receptors negative**. mastectomy, focally prominent histiocytic infiltrate c/w treatment effect, no residual carcinoma, **2/14 lymph nodes positive** for metastatic ductal carcinoma - high grade, **pathologic stage ypTX; N1a**; MX (DCIS of left side), glandular parenchyma.

**47-11-03-A032d** - (same patient as 46-11-03-A031d) - **adjacent uninvolved** normal breast tissue.

**49-11-04-A002g** - (same patient as 48-11-04-A001g), **uninvolved breast tissue**, fibrocystic changes.

**Breast tissue exhibiting no apparent pathology, derived from patients with known predisposition to breast malignancy:**

**34-10-06-A064c** - 34 yowf, normal, **prophylactic**, fibrocystic changes, **apocrine metaplasia**, microcysts, no evidence malignancy, **strong family history breast cancer,** lobulated fatty parenchyma, minimal to moderate white glandular parenchyma, no gross lesions.

**35-10-06-A070d** - 38 yowf, normal, **prophylactic,** fibrocystic changes, stromal fibrosis, focal microcalcifications, no malignancy, **history of cancer contralateral breast, BRCA 1 / 2 positive**.

**36-10-06-A103c** - 29 yowf, **normal**, increased risk, **BRCA1 positive**, lobulated fatty parenchyma, finely granular breast parenchyma, minimal fatty tissue.

**37-10-07-A026d** - 41 yowf, normal, fibrocystic changes, **prophylactic, benign, strong family history breast cancer**, fatty parenchyma, glandular parenchyma, no gross lesions, blue domes cysts up to 0.5 cm.

**38-10-07-A031a** - 43 yowf, **normal, prophylactic**, fibrocystic changes, **BRCA1-positive**, **mother with breast cancer**, lobulated fatty parenchyma, glandular.

**Normal (control) breast tissues from patients with no known pathology (i.e. reduction mammoplasty):**

**31-10-04-A001d** - 32yobf, **normal, reduction**.

**41-10-09-A133c** - 57 yowf, **normal, reduction** - benign, mild fibrocystic change, lobular fibroadipose.

**43-10-12-A058e -** 21 yowf, **normal**, fibrocystic, **reduction**, benign, fibroadenoma.

**44-11-01-A110c -** 56 yowf, **normal, reduction,** benign, lobulated, fibrous, **massive weight loss.**

**Task 3: Investigate the potential for molecular therapeutic strategies targeting mrtl to modulate Myc and reverse the malignant phenotype in breast tumor cells.**

One of the most intriguing aspects of the genomic relationship between Myc and mrtl is that both proteins can be synthesized from the same mRNA molecule. The mrtl coding sequence is positioned upstream of the Myc coding sequence. The intervening sequence, downstream of mrtl and upstream of Myc, is thought to serve an integral purpose in regulating the efficiency of Myc translation. In particular, this region has been shown to harbor a functional internal ribosome entry site (IRES) (7-8). The IRES can remain active under circumstances in which global protein synthesis is severely curtailed, such as during mitosis or apoptosis. The IRES allows Myc translation to be regulated independently of the global controls on the overall rate of protein synthesis in the cell. The natural synthesis of mrtl from the upstream region of the c-*myc* P0 mRNA inherently places the mrtl protein in the immediate vicinity of the Myc IRES, and our northwestern and biochemical fractionation data suggest that mrtl may be capable of directly binding this sequence (1). Thus we have postulated that mrtl may regulate Myc translational efficiency by modulating activity of the IRES.

**<u>UNPUBLISHED DATA</u>:**

We have found that a series of small molecule inhibitors of IRES function can be used to inhibit Myc translation (**Figure 17**).

**<u>UNPUBLISHED DATA</u>:**

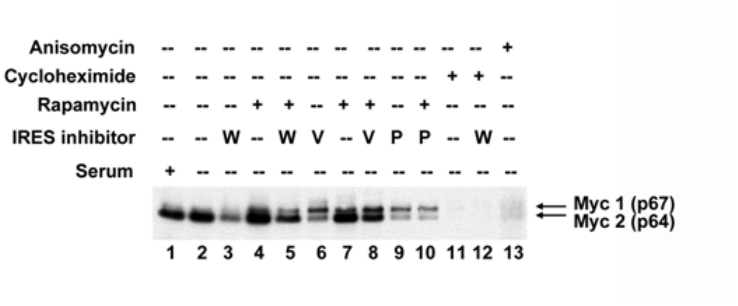


**Figure 17.** Small molecule IRES inhibitors decrease Myc protein levels and in some cases differentially alter the relative abundance of the p64 and p67 isoforms of Myc. SUM159 human breast carcinoma cells were incubated for 24 hours in the presence of translationally-active drugs as indicated. Following incubation, whole cell extracts were prepared by hot lysis, equivalent aliquots of each sample were separated by SDS / PAGE, transferred to nitrocellulose, and probed with an antibody (N262 polyclonal) to Myc. The positions of the Myc1 (p67) and Myc2 (p64) isoforms are indicated. Serum (--) = 0.5%

FCS with no supplemental insulin. Anisomycin 10 uM; Cycloheximide 100 ug/ml; Rapamycin 100 nM; IRES inhibitors W, V, P each at 10 ug / ml.

The results show that by blocking IRES activity, it is possible to induce a dramatic decrease in Myc protein levels. Exposure of cells to IRES inhibitor W results in a substantially lower overall abundance of the Myc proteins, yet p64 (Myc2) remains the predominant isoform. In contrast, in cells treated with IRES inhibitors P or V, not only is the overall level of Myc protein dramatically reduced, but the p67 (Myc1) isoform becomes dominant over p64 (Myc2). This reversal of the p64:p67 ratio is potentially very significant, because p67 has been associated with growth inhibitory / pro-apoptotic or tumor suppressor activity, whereas p64 is attributed the well-known growth-promoting and oncogenic activities associated with the c-*myc* locus, and the balance between the p67 and p64 isoforms is highly relevant to cellular homeostasis and Myc oncogenesis (9-11). In association with the decrease in Myc protein level and reversal of the p64:p67 ratio, the treated cells exhibit delayed (subacute) apoptotic death, resulting in essentially complete elimination of the tumor cell population. Intriguingly, we find that non-malignant human mammary epithelial cells (HMEC) are relatively tolerant of the IRES inhibitors, suggestive of a favorable therapeutic window inherent to this approach.

**KEY RESEARCH ACCOMPLISHMENTS:**

-- Establishment of two complex series of extensive Myc / mrtl expression and reporter constructs, requiring innovative strategies and protocols.

-- Testing of ectopic expression of mrtl from construct containing native P0 promoter and natural origin of replication positioned upstream of mrtl.

-- Acquisition and initial assessment of a total of 51 human breast surgical specimens from 46 different patients, including 18 primary invasive ductal / lobular breast carcinomas, 7 metastatic lesions of breast tumor origin (nodal metastases as well as distant metastases are represented), 5 histologically-normal specimens from genetically predisposed individuals undergoing prophylactic surgery, and 18 normal tissue specimens obtained at reduction mammoplasty.

-- Performed comprehensive analysis of mrtl coding sequence in 22 primary breast tumor specimens, metastatic lesions of breast tumor origin, non-malignant breast tissues, and human breast cells in culture, identifying codon 79 polymorphism.

-- Begun to analyze, for the first time, relative abundance of Myc and mrtl proteins in primary human breast tumor specimens, metastatic lesions of breast tumor origin, and non-malignant breast tissues, with preliminary indication that p67 (Myc1) isoform of Myc may predominate in normal breast tissues, while mrtl may be overexpressed in breast metastases.

-- First evidence of ability to modulate Myc protein levels using pharmacological reagents targeting the IRES.

REPORTABLE OUTCOMES:

Thus far, we have developed a number of the key constructs necessary for assessment of the functional relationship between mrtl and Myc. We have accumulated high quality sequence data for the mrtl coding sequence in a wide variety of primary human breast specimens. Work is ongoing to investigate the consequences of site-directed mutations of the mrtl coding sequence on Myc translation and nuclear localization. We are continuing to acquire and analyze new human breast surgical specimens for the status of Myc and mrtl and their relationship to the malignant and/or metastatic phenotype. We are continuing to investigate the consequences and implications of pharmacological modulation of Myc IRES activity and its impact on the Myc / mrtl relationship and breast tumor cell phenotype and viability.

Our work was presented in poster form at the 6th Era of Hope Conference in Orlando, August 4, 2011. Choi, H.S., Frost, A.R., Zinn, K.R., Jackson, N.L., Shaw, D.R., and Blume, S.W. (2011) Elucidating the functional relationship between mrtl and Myc and its contribution to human breast cancer pathogenesis. *Era of Hope Department of Defense Breast Cancer Research Meeting.* Abstract P44-8.

**CONCLUSION:**

Our findings continue to support the concepts that the functional relationship between mrtl and Myc and the control of Myc expression at the translational level may be critically involved in human breast cancer pathogenesis, and may be amenable to therapeutic intervention. Dramatic variations in mrtl and Myc levels in the metastatic breast tissues suggest that a major alteration in mrtl expression and Myc regulation may accompany the acquisition of the metastatic phenotype. Strategic targeting of mrtl and Myc IRES function may be capable of favorably modulating the malignant phenotype. These studies have the potential to reveal very important new information relevant to the natural history of human breast cancer, and the molecular mechanisms by which the Myc / mrtl locus contributes to this disease. By modulating activity of the Myc IRES, mrtl may differentially influence synthesis of the two Myc isoforms in the context of the P0 mRNA. Regulation of Myc expression by mrtl introduces a new perspective on the c-*myc* locus and its involvement in breast tumorigenesis, and the clinical relevance and potential therapeutic implications of these findings could be quite significant.

REFERENCES:

1. Choi, H., Jackson, N.L., Shaw, D.R., Emanuel, P.D., Liu, Y.L., Tousson, A., Meng, Z. and Blume, S.W. (2008) mrtl-A translation/localization regulatory protein encoded within the human c-myc locus and distributed throughout the endoplasmic and nucleoplasmic reticular network. *J Cell Biochem*, **105**, 1092-1108.

2. Gazin, C., Dupont de Dinechin, S., Hampe, A., Masson, JM., Martin, P., Stehelin, D., Galibert, F. (1984) Nucleotide sequence of the human c-myc locus: Provocative open reading frame within the first exon. *EMBO J.* **3**: 383-387.

3. Waltz, S.E., Trivedi, A.A. and Leffak, M. (1996) DNA replication initiates non-randomly at multiple sites near the c-myc gene in HeLa cells. *Nucleic Acids Res*, **24**, 1887-1894.

4. Sudo, K., Ogata, M., Sato, Y., Iguchi-Ariga, S.M. and Ariga, H. (1990) Cloned origin of DNA replication in c-myc gene can function and be transmitted in transgenic mice in an episomal state. *Nucleic Acids Res*, **18**, 5425-5432.

5. Miller, T.L., Huzel, N.J., Davie, J.R. and Murphy, L.C. (1993) C-myc gene chromatin of estrogen receptor positive and negative breast cancer cells. *Mol Cell Endocrinol*, **91**, 83-89.

6. Veyrune, J.L., Campbell, G.P., Wiseman, J., Blanchard, J.M. and Hesketh, J.E. (1996) A localisation signal in the 3' untranslated region of c-myc mRNA targets c-myc mRNA and beta-globin reporter sequences to the perinuclear cytoplasm and cytoskeletal-bound polysomes. *J Cell Sci*, **109 ( Pt 6)**, 1185-1194.

7. Stoneley, M., Paulin, F.E., Le Quesne, J.P., Chappell, S.A. and Willis, A.E. (1998) c-Myc 5' untranslated region contains an internal ribosome entry segment. *Oncogene*, **16**, 423-428.

8. Nanbru, C., Lafon, I., Audigier, S., Gensac, M.C., Vagner, S., Huez, G. and Prats, A.C. (1997) Alternative translation of the proto-oncogene c-myc by an internal ribosome entry site. *J Biol Chem*, **272**, 32061-32066.

9. Hann, S.R., King, M.W., Bentley, D.L., Anderson, C.W. and Eisenman, R.N. (1988) A non-AUG translational initiation in c-myc exon 1 generates an N-terminally distinct protein whose synthesis is disrupted in Burkitt's lymphomas. *Cell*, **52**, 185-195.

10. Hann, S.R., Dixit, M., Sears, R.C. and Sealy, L. (1994) The alternatively initiated c-Myc proteins differentially regulate transcription through a noncanonical DNA-binding site. *Genes Dev*, **8**, 2441-2452.

11. Benessayag, C., Montero, L, Colombie, N., Gallant, P., Cribbs, D., and Morello, D. (2005) Human c-Myc isoforms differentially regulate cell growth and apoptosis in Drosophila melanogaster. *Mol Cell. Biol.* **25**: 9897-9909.